



Repositorio Institucional de la Universidad Autónoma de Madrid

<https://repositorio.uam.es>

Esta es la **versión de autor** del artículo publicado en:

This is an **author produced version** of a paper published in:

Advanced Synthesis and Catalysis 362.6 (2020): 1345-1355

DOI: <https://doi.org/10.1002/adsc.201901465>

Copyright: © 2020 Wiley - VCH Verlag GmbH & Co. KGaA, Weinheim

El acceso a la versión del editor puede requerir la suscripción del recurso

Access to the published version may require subscription

Boron Dipyrromethene (BODIPY) as Electron-Withdrawing Group in Asymmetric Copper-Catalyzed [3+2] Cycloadditions for the Synthesis of Pyrrolidine-Based Biological Sensors

Thomas Rigotti,^{a,f} Juan Asenjo-Pascual,^{a,f} Ana Martín-Somer,^b Paula Milán Rois,^c Marco Cordani,^c Sergio Díaz-Tendero,^{b,d,e} Álvaro Somoza,^c Alberto Fraile^{a,d,*} and José Alemán^{a,d,*}

^a Department of Organic Chemistry (module 01), Universidad Autónoma de Madrid, Cantoblanco, 28049 Madrid, Spain. Webpage: www.uam.es/jose.aleman. E-mail: alberto.fraile@uam.es; jose.aleman@uam.es

^b Department of Chemistry (module 13), Universidad Autónoma de Madrid, Cantoblanco, 28049 Madrid, Spain.

^c IMDEA Nanociencia, Cantoblanco, 28049 Madrid, Spain.

^d Institute for Advanced Research in Chemical Sciences (IAChem), Universidad Autónoma de Madrid, 28049 Madrid, Spain.

^e Condensed Matter Physics Center (IFIMAC), Universidad Autónoma de Madrid, Cantoblanco, 28049 Madrid, Spain.

Abstract. In this work, we describe the use of Boron Dipyrromethene (BODIPY) as electron-withdrawing group for activation of double bonds in asymmetric copper-catalyzed [3+2] cycloaddition reactions with azomethine ylides. The reactions take place under smooth conditions and with high enantiomeric excess for a large number of different substituents, pointing out the high activation of the alkene by using a boron dipyrromethene as electron-withdrawing group. Experimental, theoretical studies and comparison with other common electron-withdrawing groups in asymmetric copper-catalyzed [3+2]

cycloadditions show the reasons of the different reactivity of the boron dipyrromethene derivatives, which can be exploited as a useful activating group in asymmetric catalysis. Additional experiments show that the so obtained pyrrolidines can be employed as biocompatible biosensors, which can be located in the endosomal compartments and do not present toxicity in three cell lines.

Keywords: asymmetric catalysis; pyrrolidines; Electron-Withdrawing Group; bioimaging cell; Frontier Molecular Orbitals; BODIPY; cycloaddition

Introduction

Boron dipyrromethene derivatives (BODIPYs) are a very remarkable family of fluorescent dyes that have been employed as powerful tools for labeling strategies in biochemistry and molecular biology.^[1] The reasons for their success are related to their high cell permeability, impressive spectroscopic properties^[2] as well as excellent robustness and chemical- and photo-stability.^[2a,3] Owing to their unique optical and chemical properties, BODIPYs have been used as biological sensors and for cell imaging. However, although some recent methodologies allow the direct labelling of biomolecules with the BODIPY unit,^[4] generally, it is necessary to use approaches that are based on conventional coupling reactions from two functionalized substrates,^[5] thus requiring tedious modifications of the target biomolecule, including the corresponding linker.

Proline and its derivatives constitute a remarkable family of natural and synthetic compounds with very interesting chemical and bioactive applications.^[6] Furthermore, proline plays a crucial role in peptides by limiting their conformational freedom, which

modulates the nucleation of their secondary structures. Those spatial arrangements tune their biological behavior and protect them against degradation. Such changes are especially relevant in therapeutic peptides, where their selectivity and activity can be enhanced.^[7] Moreover, proline core is present in the structure of kainoid natural neurotoxins such as α -Kainic acid (I),^[8] (-)-Domoic acid (II),^[9] and Acromelic acid (III),^[10] which promote potent stimulation of the central nervous system, cause brain damage, and neurological disorders (Figure 1). Another related family of synthetic molecules such as IV^[11] has been identified as potent hepatitis C virus (HCV) inhibitors (Figure 1).

Plenty of novel strategies and methods have been developed in recent years to synthesize these heterocycles. Among them, catalytic asymmetric 1,3-dipolar cycloadditions of azomethine ylides with activated alkenes have turned out to be one of the most straightforward and efficient methods for the preparation of enantioenriched prolines,^[12] from which, and by simple transformations, it is possible to obtain highly functionalized pyrrolidines.^[13]

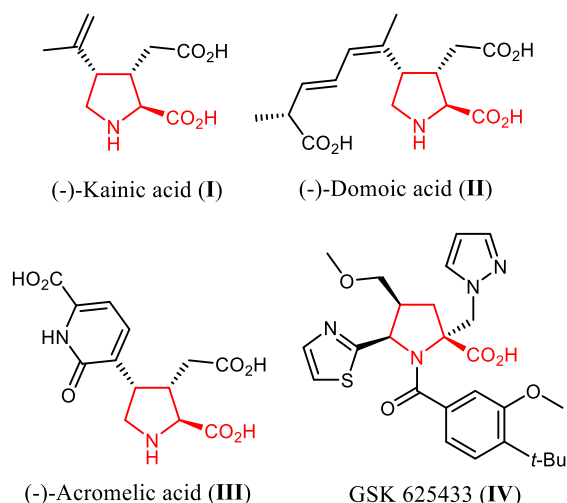


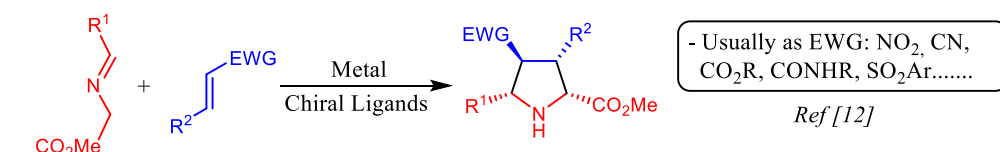
Figure 1. Different biologically active proline derivatives described in the literature.

Usually, strong electron-withdrawing groups (EWG) (e.g. nitro, ester, sulfone, amide, phosphonate, etc) at the alkene are needed to achieve the desired reactivity (Scheme 1a). In a very recent report, the activation of a double bond was achieved by a very electron-poor aryl group, such as nitrophenyl styrenes,

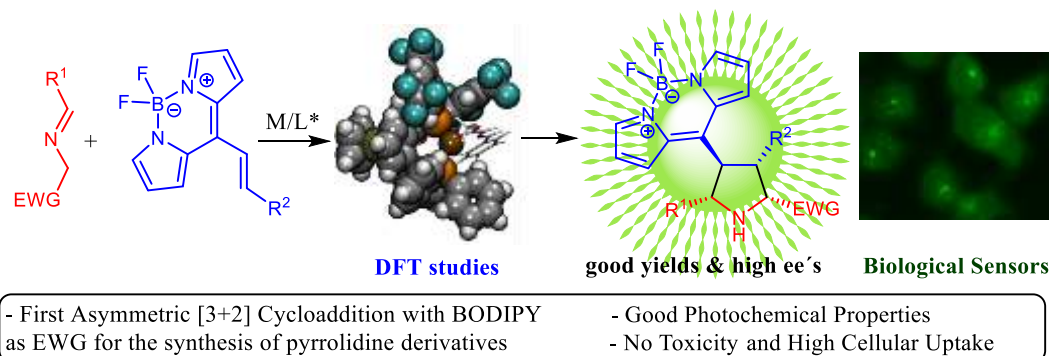
allowing their use as dipolarophiles in [3+2] cycloadditions.^[14] Nevertheless, the range of suitable dipolarophile partners is still limited, and most of them are related to the common EWGs in asymmetric catalysis.

Since BODIPY core is known for its electron-withdrawing character,^[15] and can be used as fluorescent moiety for bioimaging techniques,^[1] we wondered if it would be possible to use this interesting group as EWG for alkene activation in asymmetric [3+2] cycloaddition reactions. Taking into account that BODIPYs and pyrrolidines moieties are very important structures, this [3+2] cycloaddition will give access to enantiomerically enriched pyrrolidines incorporating a fluorophore dye (Scheme 1b). In this work, we show that BODIPY units can be used as EWG in asymmetric catalysis for the synthesis of pyrrolidines thus adding a new EWG to the range of suitable dipolarophiles in [3+2] cycloaddition reactions. Quantum chemistry calculations, comparing the reactivity with other common EWGs, demonstrate that BODIPY is able to activate the double bond better than any other. Besides, we show that the so obtained pyrrolidines incorporating a fluorophore moiety (BODIPY) could be applied to live-cell imaging in three different cellular cell lines.

a EWGs in [3+2] Cycloaddition Reactions



b This work: novel Asymmetric [3+2] Cycloaddition using BODIPY as EWG



Scheme 1. Comparison of the previously used approaches and present work (M/L*: Metal/Chiral Ligands).

Results and Discussion

Synthesis of BODIPY pyrrolidines, screening and scope. We began our investigations carrying out the cycloaddition reaction between iminoester **1a** and alkenyl-BODIPY **2a** in the presence of

[Cu(CH₃CN)₄][PF₆] (15 mol%), triethylamine (30 mol%) as base, toluene as solvent and several chiral ligands (**L1-L6**) (15 mol%) at room temperature (Table 1, entries 1-6). It should be noted that in all trials a complete *exo* selectivity was obtained (*dr*>98:2). The best result was achieved using Walphos (**L6**) as the ligand (entry 6, Table 1), obtaining the *exo*-**3a** adduct in 90% *ee* and complete

diastereoselectivity ($dr > 98:2$) but with low yield. In order to improve this result, we tested different solvents (see S.I. for further details), obtaining the desired product in 85% yield and with a 96% of enantiomeric excess (ee) when the reaction was performed in DCM (entry 7). Then, the influence of the catalyst loading on the reaction outcome was evaluated. The use of 10 mol% of catalyst maintained the ee values previously obtained (entry 8), but a

lower catalytic loading (5 mol%) provoked a slight decrease in the final enantioselectivity (90% ee , entry 9, Table 1). Considering these results, we decided to decrease the temperature to 4 °C, achieving the final adduct *exo*-**3a** in high yield (89%) and excellent enantioselectivity (98%) (entry 10, table 1).^[16] However, the use of even lower catalyst loading (2.5 mol%, entry 11, table 1) gave low ee .

Table 1. Catalysts screening and optimization of reaction conditions.^[a]

Chemical structures of catalysts L1-L6:

- (R)-DTBM-Segphos (L1)**: Ar = 4-MeO-3,5-(*t*-Bu)₂C₆H₂
- (R)-Garphos (L2)**: Ar = 3,5-(CF₃)₂C₆H₃
- (R)-BINAP (L3)**
- (R)-Josiphos (L4)**
- (R)-Fesulphos (L5)**
- (R)-Walphos (L6)**: Ar = 3,5-(CF₃)₂C₆H₃

Entry	L (%mol)	Solvent	T (°C)	Yield (%) ^[c]	Exo/endo ^[d]	ee (%) ^[e]
1	L1 (15)	Toluene	25	64	>98:2	-84
2	L2 (15)	Toluene	25	58	>98:2	6
3	L3 (15)	Toluene	25	60	>98:2	-75
4	L4 (15)	Toluene	25	49	>98:2	-70
5	L5 (15)	Toluene	25	34	>98:2	-76
6	L6 (15)	Toluene	25	33	>98:2	90
7	L6 (15)	DCM	25	85	>98:2	96
8	L6 (10)	DCM	25	nd	>98:2	97
9	L6 (5)	DCM	25	nd	>98:2	90
10	L6 (5)	DCM	4	89	>98:2	98
11	L6 (2.5)	DCM	4	nd	>98:2	90

^[a] All the reactions were performed on a 0.07 mmol scale of **2a** using a dry solvent (0.5 mL) under air atmosphere. ^[b] CuPF₆: [Cu(CH₃CN)₄][PF₆]. ^[c] Isolated yield after flash-chromatography. ^[d] Ratio determined by ¹H NMR spectroscopy of the crude mixture. ^[e] Determined by chiral HPLC.

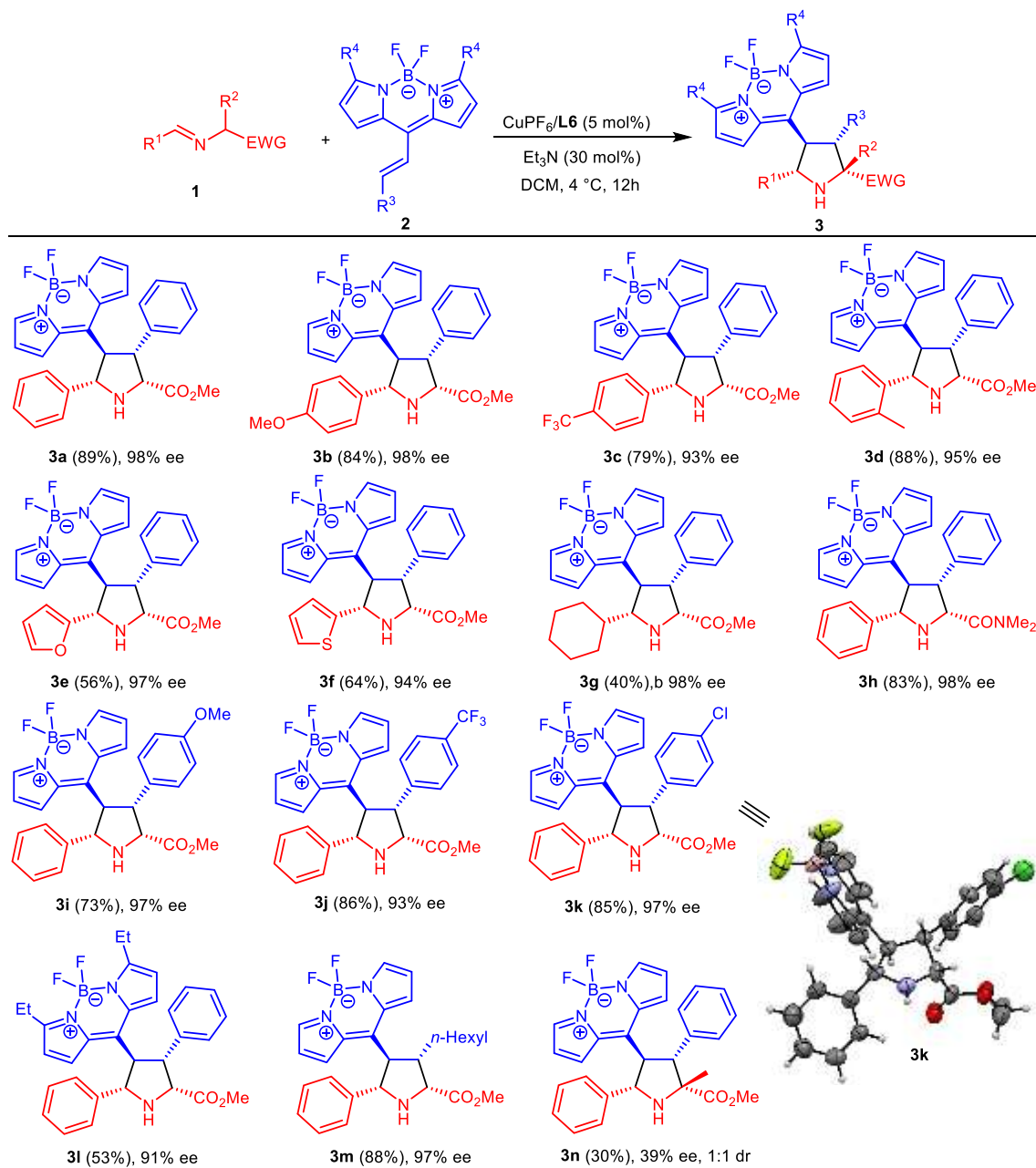
Once the best conditions were determined (entry 10, Table 1), we carried out the scope of the reaction using different iminoesters **1** and alkenyl-BODIPYs **2** (Table 2). Firstly, we tested the influence of the electronic properties and the steric effect of substituents at the dipole precursor **1**. The presence of an electron-donating group (EDG, *p*-MeO, **1b**) or an EWG (*p*-CF₃, **1c**) in the aryl moiety yielded pyrrolidines **3b-c** in high yield (79-84%) and high ee (93-98%), which indicates that the reaction tolerates

imines with different electronic properties. A more sterically hindered imine such as **1d** allowed the synthesis of **3d** with excellent enantioselectivity and without erosion of the final yield (88%). Similarly, the cycloaddition reactions of imines **1e-f**, containing a heteroaromatic ring, gave the corresponding adducts **3e** and **3f** with high ee . The reaction also proceeded with very high enantioselectivity (98% ee) but with a lower yield (40%) with the cycloalkyl substituent (**1g**). The reaction worked properly even

when the ester group of the imine was substituted for an amide group, obtaining the pyrrolidine **3h** in very high yield and excellent *ee* (83% yield, 98% *ee*). Then, a variety of different alkenyl-BODIPYs **2d-f** were also studied (third and fourth row). Indeed, electron-donating and electron-withdrawing groups on the aryl moiety of the dipolarophile were tolerated, leading to pyrrolidines **3i** (*p*-MeO), **3j** (*p*-CF₃) and **3k** (*p*-Cl) with very high enantioselectivities (93-97%

ee). The presence of two ethyl groups at C-3 and C-5 positions of the BODIPY core did not affect the stereoselectivity (91% *ee*) but provoked a decrease of the yield (53%). Finally, we were delighted to find that alkenyl-BODIPY **2f**, which contains a primary alkyl chain substituent, also led to the pyrrolidine **3m** in high yield and very high enantioselectivity. In addition, pyrrolidine **3n** with a quaternary center was obtained, but in low yield and enantiomeric excess.

Table 2. Scope for the synthesis of BODIPY pyrrolidines **3** from different imines **1** and double bonds **2**.^[a]



The spatial arrangement of all the substituents of the pyrrolidine moiety was determined from the absolute configuration of the asymmetric centers of pyrrolidine **3k**, which was unequivocally assigned as

2*R*, 3*R*, 4*R*, 5*S* by X-Ray crystallographic analysis (see bottom-right, Table 2).^[17] This configuration can be explained by an *exo* approach, (the more favorable when copper salts are used)^[12b] of the dipolarophile **2**

to the bottom prochiral face (2*Re*,4*Si*) of dipole **1** (see explanation in next section).

DFT calculations: BODIPY as EWG, thermodynamics and kinetics.^[18] In order to shed light into the reaction mechanism, additional experiments and DFT calculations were carried out.^[19] We modeled the reaction between dipole **1a** and dipolarophile **2a** in the presence of the catalyst complex: [Cu(CH₃CN)₄][PF₆]/Walphos (Cu/**L6**). We started the computational study analyzing the most

favorable way for the dipole to coordinate to the catalyst complex. As it can be seen in Figure 2a, once the metalloazomethine ylide is formed in presence of the base (dipole), it can coordinate with Cu/**L6** in two different ways: complex **I** or **II**; both of them having the top prochiral face blocked by the 3,5-ditrifluoromethylaryl substituents of the Walphos ligand. The Gibbs free energy difference (ΔG) between **I** and **II** is 4.15 kcal/mol, being complex **I** the most stable.

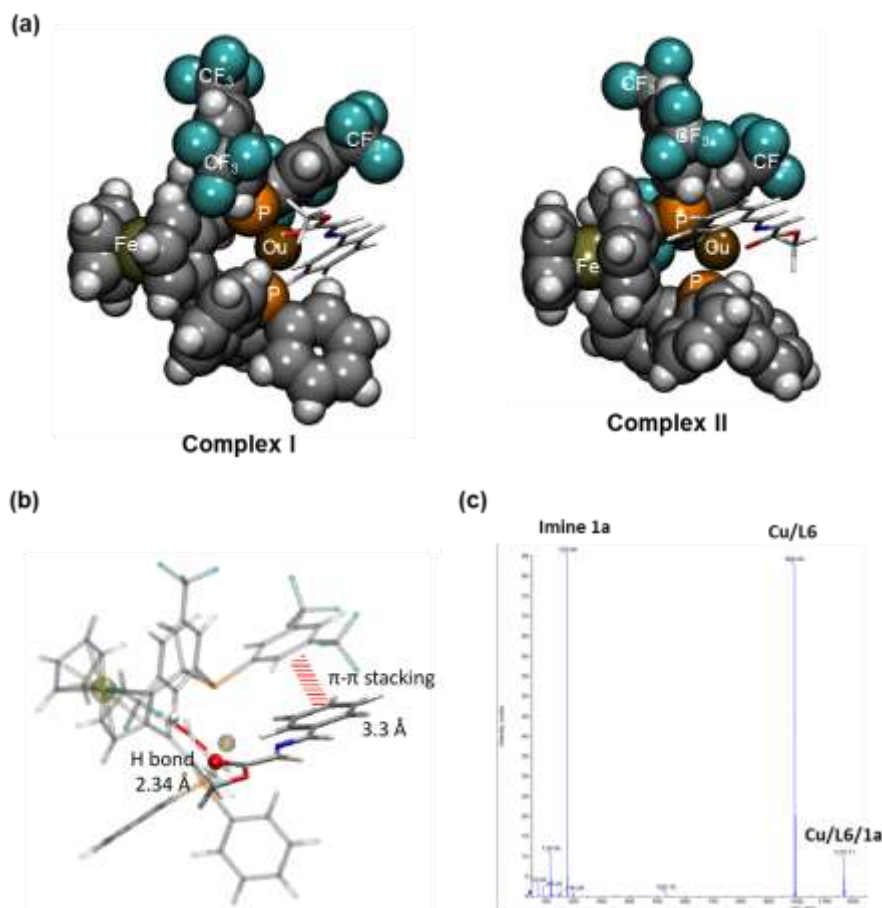


Figure 2. a) Optimized structures (at B3LYP/6-31G(d,p) level of theory) for the two possible orientations of the complex between the catalyst and dipole: Cu/**L6**/dipole (see Figure S4 in the Supporting Information for more details). The Gibbs free energy difference (ΔG) between them is 4.15 kcal/mol, being complex **I** the most stable. b) Stabilizing interactions present in complex **I**. c) Mass spectrum of a mixture of Cu, ligand **L6** and imine **1a** (see S.I. for full mass-spectrum).

This could be attributed to a stabilizing π - π interaction between the phenyl group of the imine and a 3,5-(CF₃)₂Ph ring of the ligand, which is absent in complex **II** (Figure 2b). In addition, an intramolecular hydrogen bond between the carbonyl oxygen of the imine and a hydrogen of the other 3,5-(CF₃)₂Ph ring of the ligand could further stabilize complex **I**. In order to check that a complex Cu/**L6**/**1a** was formed and stable, we carried out a mass spectroscopy study (see Supporting Information). We detected a peak at *m/z* 1170.11 amu corresponding to the Cu/**L6**/**1a** complex and a peak at

m/z 993.04 amu, which corresponds to the Cu/**L6** complex (Figure 2c). This evidences the existence and stability of the Cu/**L6**/**1a** complex.

In a second step, we studied the attack of several dipolarophiles to the previously formed dipole-catalyst complex (complex-**I**). Frontier Molecular Orbital Theory is often employed to explain the reactivity on this kind of reactions.^[20] Thus, the HOMO-LUMO gap energy difference between the HOMO of the dipole and the LUMO of the dipolarophile can be related to the reaction rate constant, being faster the reaction as the HOMO-

LUMO gap decreases. Experimental conversions,^[21] after 30 minutes at r.t., and values of HOMO-LUMO gap for different dipolarophiles are shown in Figure 3

together with the LUMO of the dipolarophiles considered.

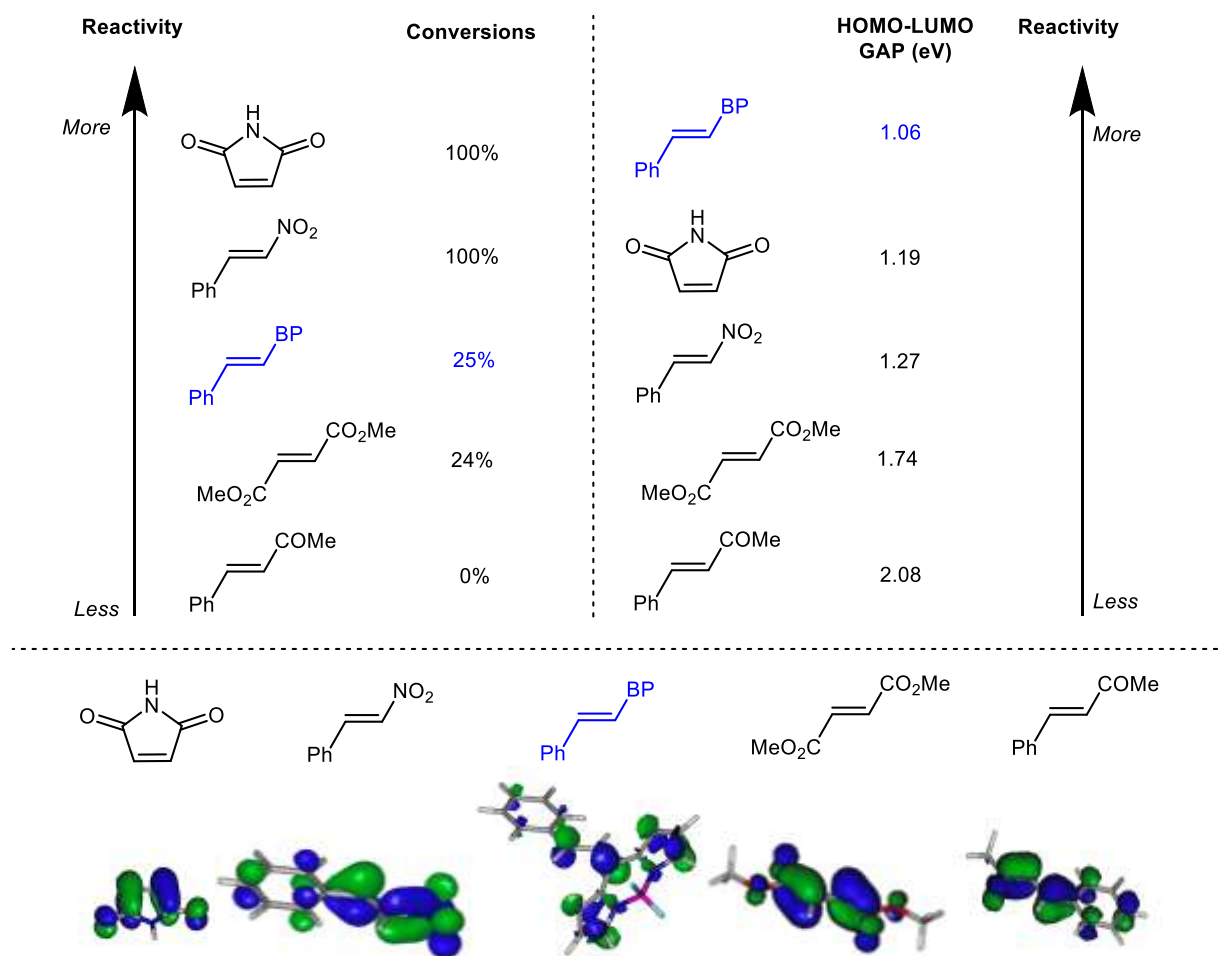


Figure 3. Conversions and HOMO-LUMO gap for the reaction of Cu/**L6**/dipole with different dipolarophiles. We have used Kohn-Sham orbitals computed at B3LYP/6-31G(d,p) level of theory. The LUMO of the different dipolarophiles is also shown in the bottom.

In general, we found a good correspondence between conversion and HOMO-LUMO gap. However, for the derivative **2a** with the BODIPY unit as EWG, the low HOMO-LUMO gap (1.06 eV) does not correspond to the low conversion found experimentally (25%). The BODIPY is a better EWG than the nitro group since it triggers a larger decrease of the LUMO energy than the nitro group (and consequently the HOMO-LUMO gap is smaller for the BODIPY derivative). However, conversion to product is one quarter of that obtained with β -nitrostyrene. Therefore, these differences between

LUMO and HOMO cannot explain the observed trend and other factors must influence the reactivity, affecting the conversion.

This leads us to evaluate whether kinetic factors control the reactivity. Figure 4a shows the potential energy surface (PES) for the [3+2] cycloaddition reaction of ylide **1a** with **2a** in the presence of catalyst (Cu/**L6**). Figure 4b shows the corresponding PES using β -nitrostyrene as dipolarophile in the presence of catalyst (Cu/**L6**) and ylide **1a**. Therefore, a direct comparison of the reaction of BODIPY **2a** and β -nitrostyrene with **1a** is shown (Figure 4).

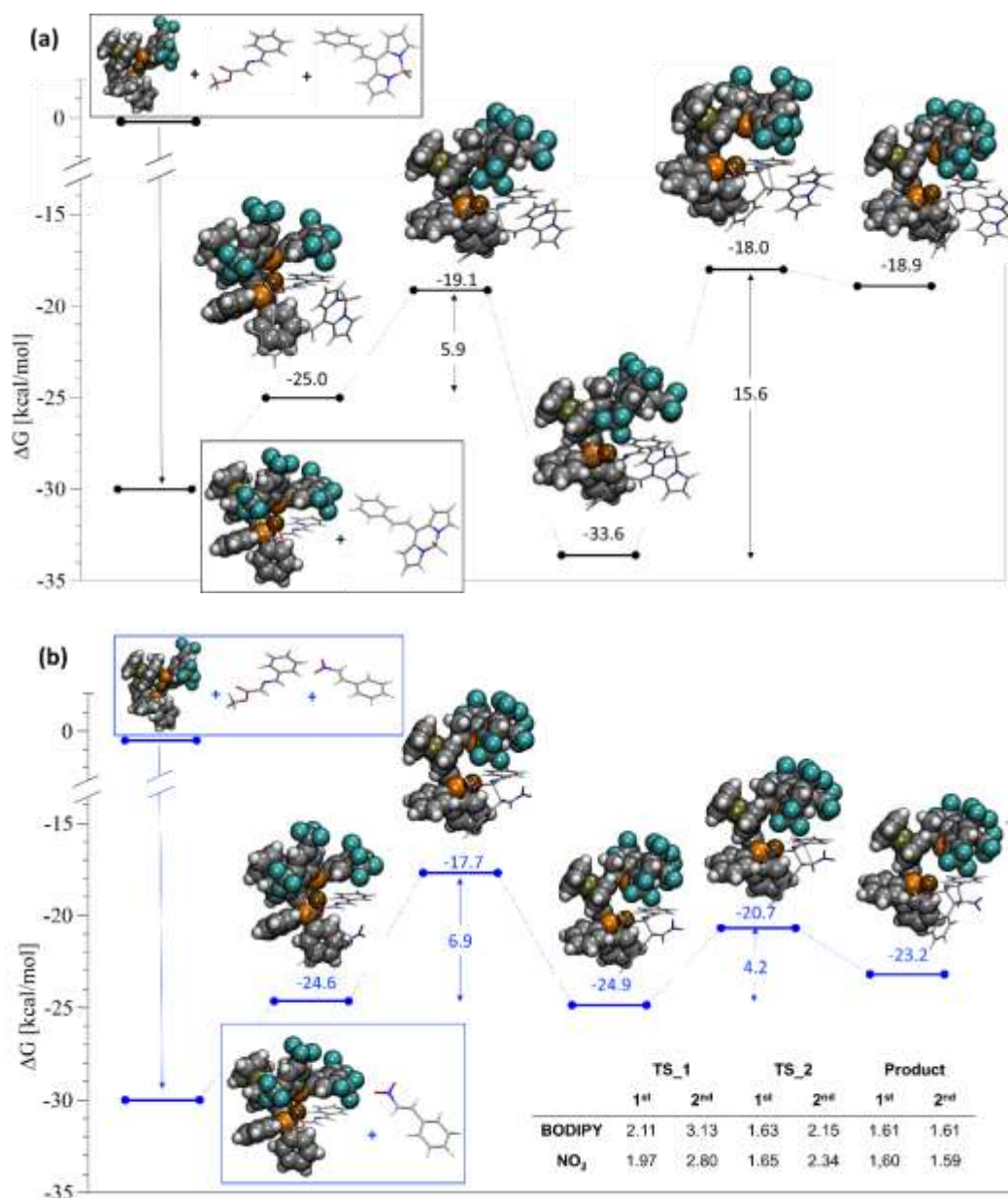


Figure 4. Potential energy surface for the [3+2] cycloaddition reaction of ylide **1a** in the presence of catalyst (CuPF₆/L6) with BODIPY alkene **2a** (a), or with β -nitrostyrene (b). PES computed at SMD(Dichloromethane)/wB97X-D/6-311+G(d,p)//B3LYP/6-31G(d,p) level of theory. Relative Gibbs free energies are referred to the separate reactants (ylide **1a**, catalyst and dipolarophile ((a) BODIPY alkene **2a**, (b) β -nitrostyrene)). From left to right: separate reactants, PAC, 1st transition state (TS), intermediate, 2nd TS and final pyrrolidine product. A table with the distances of the 1st and 2nd C-C forming bonds for key structures is also shown.

The zero corresponds to the separated catalyst, dipole and dipolarophile. The first step is the exothermic formation of complex **I** between the catalyst and the dipole (Cu/L6/ylide-**1a**) as previously stated, which is 30 kcal/mol more stable than the separate reactants. Then, complex **I** forms, together with the dipolarophile (**2a** or β -nitrostyrene), a pre-association complex (PAC),^[22] which is about 5 kcal/mol above in energy.

The mechanism for BODIPY substituted alkene **2a** and β -nitrostyrene is qualitatively similar. The [3+2]

cycloaddition reaction is stepwise in both cases. Thus, the first energy barrier corresponds to the formation of the first new C-C bond leading to an intermediate. The second energy barrier corresponds to cyclization of the intermediate through the formation of a 2nd C-C bond, yielding the final products. Also in both cases this second step is reversible since the product is less stable than the intermediate. However, there are several quantitatively essential differences between the reaction mechanisms of the two considered dipolarophiles. For BODIPY derivative, the rate-

limiting step is the formation of the 2nd C-C bond. On the contrary, for β -nitrostyrene, the highest barrier corresponds to 1st C-C bond formation being this the rate-limiting step.

The intermediate is markedly more stable for **2a** (BODIPY) than for β -nitrostyrene. Moreover, β -nitrostyrene intermediate has about the same energy as the PAC while BODIPY intermediate is significantly more stable than its PAC (about 9 kcal/mol). This could be explained by the more significant charge separation found for the BODIPY derivative (see Figure S5 in the Supporting Information). Since BODIPY is a better EWG than nitro, the negative charge located in the alkene moiety is larger for the first one (0.74 vs. 0.60, respectively). Concomitantly, the positive charge located in the catalyst moiety is equivalently more substantial. The greater charge separation leads to a more significant dipole moment in the BODIPY alkene (21.6 D vs. 16.2 D) and a larger electrostatic stabilization of the BODIPY intermediate.

We can also explain these quantitative differences using the orbital picture. Thus, the 1st step is favored for BODIPY **2a** because the HOMO-LUMO gap is smaller (1.06 vs. 1.27 eV for **2a** and nitrostyrene, respectively). However, this interaction leads to the formation of a very stable intermediate compared to β -nitrostyrene. In addition, orbital overlap for formation of the product from the intermediate (2nd C-C bond) is much better for β -nitrostyrene (see Figure 5), making this process -and the overall reaction- faster for the latter one. Furthermore, β -nitrostyrene product is more stable than BODIPY product **3a**. Probably due to higher steric congestion at the BODIPY product.

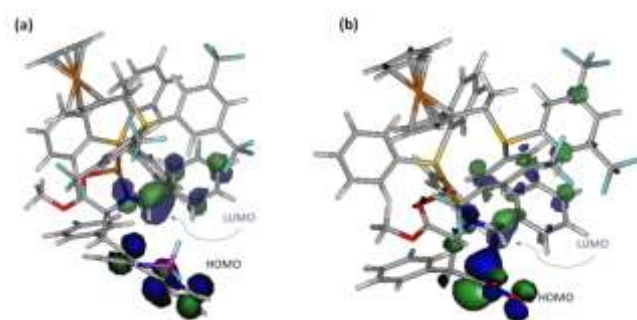


Figure 5. Frontier molecular orbitals in the intermediate of the reaction pathway computed at the B3LYP/6-31G(d,p). (a) BODIPY alkene **2a**; (b) β -nitrostyrene.

Overall, BODIPY is able to activate the double bond in the first C-C bond formation better than other typical EWGs used for [3+2] cycloaddition reactions in spite of its bulkiness. However, the second C-C bond requires more energy due to the high stabilization of the intermediate provided by the BODIPY group.

BODIPY pyrrolidine derivatives as probes for imaging. Taking into account that the synthesized

pyrrolidines-BODIPYs **3a-n** showed excellent absorption and emission properties (see Figure 7b), similar to those described in the literature for other BODIPY derivatives,^[3] we thought that it would be very interesting to evaluate the applicability of these pyrrolidine-BODIPYs **3** for live-cell imaging. We interrogated representative derivatives (**3a** and **3h**) for their ability to penetrate in three cellular lines, MEL 202 (uveal melanoma cell line), PANC-1 (pancreatic cancer cell line) and MCF7 (breast cancer cell line), and their propensity for nonspecific background staining. The results obtained with BODIPYs **3a** and **3h** were compared with the derivative **4**,^[23] to determinate the influence of the pyrrolidine moiety and to show the advantage of having this structure joined to the BODIPY core.

First, we studied their toxicity by incubation during 24 h in the three cell lines mentioned at different concentrations. The BODIPY derivatives **3a**, **3h** and **4** were non-toxic up to 10 μ M (Figure 6 and S6 in the Supporting Information). We observed a decrease in the viability of the cells when treated with the compounds at high concentrations (100 μ M). However, this result is due to the presence of DMSO, required to solubilize the compounds at such concentration, since the viability reduction is the same when exposed only to DMSO in the three cell lines tested. Therefore, we selected 10 μ M concentration for the next experiments.

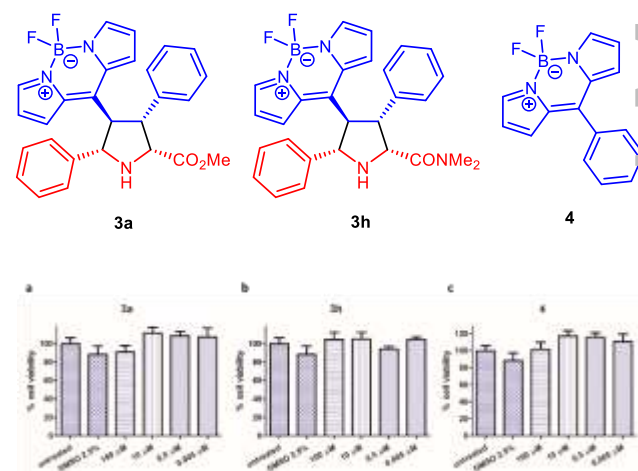


Figure 6. BODIPYs toxicity in PANC-1 cell line. The highest DMSO concentration employed was 2.5 %, the same DMSO amount present in the samples at 100 μ M concentration. (a) BODIPY **3a**, (b) BODIPY **3h**, (c) BODIPY **4**.

We studied BODIPYs accumulation in the cell using lysotracker, as an endosomal probe (Figure 7a). The images show that BODIPYs were colocalized with the lysotracker in PANC-1, revealing that BODIPYs were accumulated in endosomal compartments. Moreover, the internalization of the BODIPY derivatives was also studied by flow cytometry (Figure 7c). In this assay, the peaks at the right imply better uptake by the cells. Therefore, the

internalization in PANC-1 was higher with BODIPY **3a** than BODIPY **3h**, and the latter was better uptaken than BODIPY **4** (Figure 7c). The same

behavior was observed in MEL 202 and MCF-7 cell lines (see Supporting Information).

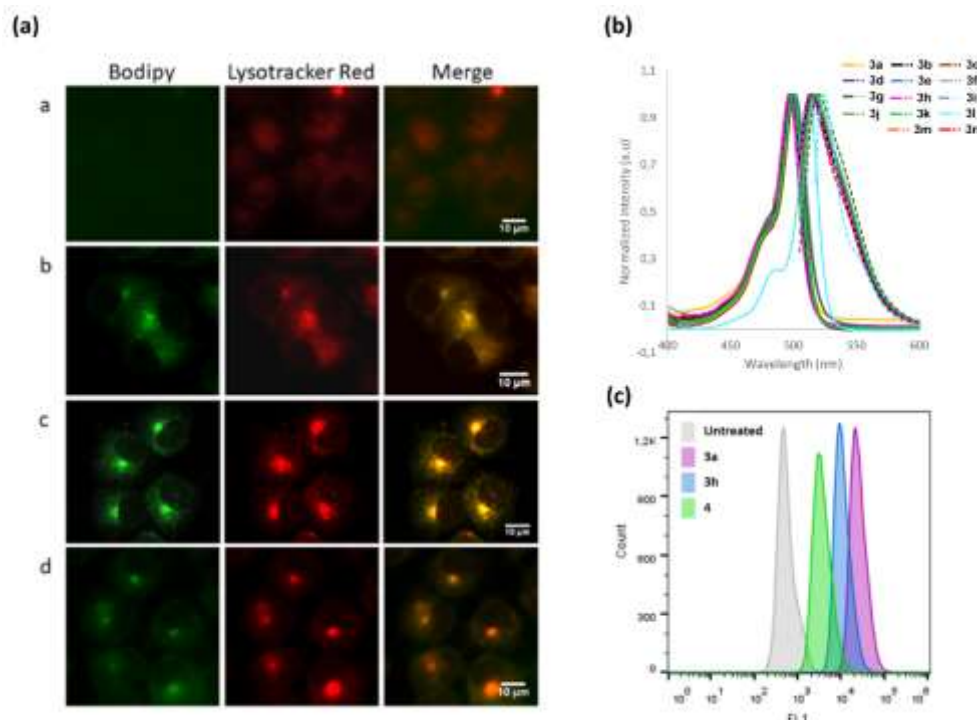


Figure 7. (a) BODIPYs localization in PANC-1 cells. In the first column, BODIPY fluorescence is showed in green, in the second one a lysotracker Red labeling to show the endosomal compartment and in the third column the merge. Row *a* corresponds to untreated PANC-1 cells. Row *b* to PANC-1 cells treated with 10 μM of BODIPY **3a**. Row *c* to PANC-1 cells treated with 10 μM of BODIPY **3h** and Row *d* to PANC-1 cells treated with 10 μM of BODIPY **4**. (b) Absorption and emission (dash-line) spectra of BODIPYs **3a-n** (see S.I. for details). (c) BODIPY uptake in PANC-1. The further to the right, the better the uptake.

This study highlights the potential use of the newly synthesized pyrrolidines-BODIPYs for imaging lysosomes in cells. All of them were localized in the endosomal compartment but the cellular uptake was very different between the different BODIPYs, obtaining the best result with the proline BODIPY **3a** in the three different tumoral cells.

Conclusion

In summary, we have reported an easy and versatile approach for preparation of pyrrolidine-BODIPY derivatives in high yields and excellent stereoselectivities by an asymmetric metal-catalyzed [3+2] cycloaddition reaction. Also, it has been shown that the BODIPY group is capable of activating double bonds in this type of reactions acting as an electron-withdrawing group. DFT studies show that, in this specific [3+2] cycloaddition, the BODIPY moiety, although it should work as a better EWG, is less reactive than a nitro group. This is because the intermediate generated in the first step of the cycloaddition is very stable in the case of the BODIPY-alkene because of the high charge

separation between the catalyst/L6/dipole complex and the dipolarophile, leading to a great electrostatic stabilization. The derivatives were tested in three different cell lines revealing a selective accumulation in the lysosomes. Therefore, due to their inherent excellent fluorescent properties, the synthesized BODIPY derivatives could be used for the imaging of these organelles in live cells.

Experimental Section

General procedure for the [3+2] cycloaddition

An oven-dried 10 mL vial equipped with a magnetic stir bar was charged with [Cu(CH₃CN)₄]PF₆ (0.005 mmol, 5 mol%), (*R*)-Walphos ligand **L6** (0.006 mmol, 6 mol%) and the corresponding BODIPY substrate **2** (0.1 mmol). Then, anhydrous DCM (0.75 mL) were added, followed by the corresponding imine **2** (0.15 mmol, 1.5 equiv). The vial was closed with a PTFE/rubber septum and the reaction mixture was stirred at 4 °C for 15 minutes prior adding triethylamine (0.03 mmol, 30 mol%). Stirring was maintained at the same temperature for 12 hours. The solvent was removed under reduced pressure and the crude mixture was purified by flash chromatography (eluent indicated in each case) affording the corresponding pyrrolidines **3**.

Methyl (2R,3R,4R,5S)-4-(5,5-difluoro-5H-4 λ ,5 λ -dipyrrolo[1,2-c:2',1'-f][1,3,2] diazaborinin-10-yl)-3,5-diphenylpyrrolidine-2-carboxylate (3a)

Pyrrolidine **3a** was obtained following the general procedure, from BODIPY **2a** and imine **1a**, after purification by flash chromatography (CyHex:EtOAc = 2:1) as a red solid (42 mg, 89% yield). $[\alpha]_D^{20} = -139$ ($c = 0.035$, CHCl₃). ¹H NMR (500 MHz, CDCl₃, 278 K): δ 7.80 (br s, 1H), 7.73 (br s, 1H), 7.62 (br s, 1H), 7.45 – 7.41 (m, 2H), 7.33 – 7.18 (m, 8H), 6.65 (br s, 2H), 6.20 (br s, 1H), 4.87 (d, $J = 9.8$ Hz, 1H), 4.68 (d, $J = 9.4$ Hz, 1H), 4.33 (t, $J = 9.5$ Hz, 1H), 3.87 (t, $J = 9.7$ Hz, 1H), 3.25 (s, 3H), 3.02 (br s, 1H). ¹³C NMR (126 MHz, CDCl₃, 278 K): δ 172.6, 148.2, 145.8, 141.8, 139.5, 139.0, 137.2, 132.3, 129.7, 129.0, 128.7, 128.5, 127.8, 127.7, 127.6, 126.4, 118.8, 118.0, 72.5, 65.9, 59.7, 58.8, 51.9. ¹⁹F NMR (282 MHz, CDCl₃, 298 K): δ -145.6 – -145.9 (m, 2F). HRMS (ESI⁺): calculated for C₂₇H₂₅BF₂N₃O₂⁺, $[M+H]^+ = 472.2002$; found = 472.2008. The enantiomeric excess was determined by HPLC on a Chiralpak IB column: *n*-Hex/*i*-PrOH 40:60, flow rate 1.0 mL/min, $\lambda = 495$ nm, $\tau_{\text{major}} = 12.06$ min, $\tau_{\text{minor}} = 7.06$ min (98% ee).

Computational details

Geometry optimizations, orbital energies, harmonic frequency calculations, thermodynamic corrections and intrinsic reaction coordinate (IRC) calculations were computed with B3LYP functional combined with Pople's double- ξ basis set 6-31G(d,p), which includes polarization functions. Harmonic vibrational frequencies were computed to characterize minima and transition states (TS) and IRCs to verify connectivity between TSs and adjacent minima at the same level of theory - B3LYP/6-31G(d,p). More accurate values for the final energies were computed by means of single point calculations with ω -B97X-D functional and a larger, triple- ξ , basis set including diffuse functions, 6-311+G(d,p), over the geometries previously optimized. The range-separated hybrid functional ω -B97X-D includes Grimme's D2 dispersion correction, absent in B3LYP functional. The effect of the solvent (CH₂Cl₂) was also taken into account using the SMD continuum solvation model.

Biological studies

Viability assays: alamar blue. After treating the cells with the solutions of the compounds, a stock solution of resazurin sodium salt (Sigma-Aldrich, St. Louis, MO, USA) (1 mg/mL) in PBS was diluted 1% (v/v) in complete RPMI medium and added to the cells. After 3 h in the incubator (37 °C), the fluorescence was measured at 25 °C in a plate reader Synergy H4 Hybrid reader (BioTEK) $\lambda_{\text{ex}} = 550$ nm, $\lambda_{\text{em}} = 590$ nm. The fluorescent intensity measurements were processed using the following equation: % Cell viability = ((Sample data - Negative control) / (Positive control - Negative control)) \times 100. The positive control corresponds with untreated cells. A resazurin solution without cells was used as negative control.

Localization assay. The cells were harvested on coverslips. Then the bodipys were added in a final concentration of 10 μ M. 24h later the cells were washed twice with PBS. Finally, 48 h after the treatment LisoTracker red DND-99 was dissolved in optiMEM to 50 nM final concentration. The solution was incubated 5 min with the cells at room temperature and the cells were then washed twice with PBS. Then, the samples were studied in a Leica DMI3000 M inverted microscope (Leica, Wetzlar, Germany) at 800 exposure units. The bodipys signal was observed with the green filter of the microscope (λ_{ex} 460-500 nm; λ_{em} 515-545 nm) and the lysotracker with the red filter (λ_{ex} 540-580 nm; λ_{em} 615-680 nm). The images were modified for a correct visualization with Fiji-Image J program.

Flow cytometry assay. After the treatment the cells were trypsinized for 5 min, then the process stopped with complete medium. The cells were washed with PBS and centrifugated with 177 \times g for 5 min in an Eppendorf centrifuge 5804 R (Eppendorf, Hamburg, Germany). The process was done twice. After that, the cells were analyzed in a Beckman Coulter Cytomics 500 Flow Cytometer (Beckman Coulter, Indianapolis, IN, USA) using 20000 cells.

Acknowledgements

This work was supported by the Spanish Government (RTI2018-095038-B-I00, CTQ2016-76061-P, SAF2017-87305-R), Comunidad de Madrid (IND2017/IND-7809), and co-financed by European Structural and Investment Fund. We acknowledge the generous allocation of computing time at the CCC (UAM). Financial support from the Spanish Ministry of Economy and Competitiveness, through the "Maria de Maeztu" Program of Excellence in R&D (MDM-2014-0377), is also acknowledged. Asociación Española Contra el Cáncer, and IMDEA Nanociencia acknowledge support from the 'Severo Ochoa' Programme for Centres of Excellence in R&D (MINECO, Grant SEV-2016-0686). F. E. and A. G. thank the Spanish Government for FPI-PhD fellowships and E.M.A for FPU-PhD fellowship. P.M.R thanks the Ministry of Economy, Industry and competitiveness of Spain for the FPI grant (BES-2017.082521). A.M.S. thanks CAM for a postdoctoral contract (2016-T2/IND-1660).

References

- [1] a) S. Kolemen, E. U. Akkaya, *Coord. Chem. Rev.* **2018**, 354, 121-134; b) S. Krajcovicova, J. Stankova, P. Dzubak, M. Hajdich, M. Soural, M. A. Urban, *Chem. Eur. J.* **2018**, 24, 4957-4966; c) R. Lincoln, L. F. Greene, W. Zhang, S. Louisia, G. Cosa, *J. Am. Chem. Soc.* **2017**, 139, 16273-16281; d) T. Kowada, H. Maeda, K. Kikuchi, *Chem. Soc. Rev.* **2015**, 44, 4953-4972; e) P. Rivera-Fuentes, S. J. Lippard, *Acc. Chem. Res.* **2015**, 48, 2927-2934; f) Y. Ni, J. Wu, *Org. Biomol. Chem.* **2014**, 12, 3774-3791.
- [2] a) G. Ulrich, R. Ziessel, A. Harriman, *Angew. Chem. Int. Ed.* **2008**, 47, 1184-1201; b) N. Boens, V. Leen, W. Dehaen, *Chem. Soc. Rev.* **2012**, 41, 1130-1172; c) A. Loudet, K. Burgess, *Chem. Rev.* **2007**, 107, 4891-4932.
- [3] N. Boens, B. Verbelen, W. Dehaen, *Eur. J. Org. Chem.* **2015**, 6577-6595.
- [4] a) W. Wang, M. M. Lorion, O. Martinazzoli, L. Ackermann, *Angew. Chem. Int. Ed.* **2018**, 57, 10554-10558; b) L. Mendive-Tapia, C. Zhao, A. R. Akram, S. Preciado, F. Albericio, M. Lee, A. Serrels, N. Kielland, N. D. Read, R. Lavilla, M. Vendrell, *Nat. Commun.* **2016**, 7, 10940.
- [5] a) P. S. Deore, D. V. Soldatov, R. A. Manderville, *Sci. Rep.* **2018**, 8, 16874; b) M. H. Y. Cheng, H. Savoie, F. Bryden, R. W. Boyle, *Photochem. Photobiol. Sci.* **2017**, 16, 1260-1267; c) N. Zhao, T. M. Williams, Z. Zhou, F. R. Fronczek, M. Sibrian-Vazquez, S. D. Jois, M. G. H. Vicente, *Bioconjugate Chem.* **2017**, 28, 1566-1579; d) L. C. D. de Rezende, F. A. da Silva Emery, *Orbital Elec. J. Chem.* **2013**, 5, 62-83.
- [6] a) A. A. Morgan, E. Rubenstein, *PLOS One* **2013**, 8, e53785; b) G. Wu, F. W. Bazer, R. C. Burghardt, G. A.

- Johnson, S. Woo Kim, D. A. Knabe, P. Li, X. Li, J. R. McKnight, M. Carey Satterfield, T. E. Spencer, *Amino Acids* **2011**, *40*, 1053-1063; c) S Kaul, S. S. Sharma, I. K. Mehta, *Amino Acids* **2008**, *34*, 315-320.
- [7] a) Y. Che, G. R. Marshall, *Biopolymers* **2006**, *81*, 392-406; b) S. M. Cowell, Y. S. Lee, J. P. Cain, V. J. Hruby, *Curr. Med. Chem.* **2004**, *11*, 2785-2798; c) P. Karoyan, S. Sagan, O. Lequin, J. Quancard, S. Lavielle, G. Chassaing in: *Targets in Heterocyclic Systems Vol. 8* (Eds.: O. A. Attanasi, D. Spinelli), RSC, Cambridge, **2004**, pp 216-273; d) C. Toniolo, M. Crisma, F. Formaggio, C. Peggion, *Biopolymers (Pept. Sci.)* **2001**, *60*, 396-419.
- [8] X.-Y. Zheng, H.-L. Zhang, Q. Luo, J. Zhu, *J. Biomed. Biotechnol.* **2011**, 2011, Article ID 457079.
- [9] O. M. Pulido, *Mar. Drugs* **2008**, *6*, 180-219.
- [10] H. Shinozaki, M. Ishida, Y. Gotoh, S. Kwak in: *Amino Acids* (Eds.: G. Lubec, G. A. Rosenthal), Springer, Dordrecht, **1990**, pp 281-293.
- [11] F. Gray, L. Amphlett, H. Bright, L. Chambers, A. Cheasty, R. Fenwick, D. Haigh, D. Hartley, P. Howes, R. Jarvest, F. Mirzai, F. Nerozzi, N. Parry, M. Slater, S. Smith, P. Thommes, C. Wilkinson, E. Williams, *42nd Meeting of the European Association for the Study of Liver Diseases*, Barcelona, Spain, April 11-15, **2007**.
- [12] a) G. Pandey, P. Banerjee, S. R. Gadre, *Chem. Rev.* **2006**, *106*, 4484-4517; b) J. Adrio, J. C. Carretero, *Chem. Commun.* **2011**, *47*, 6784-6794; c) J. Adrio, J. C. Carretero, *Chem. Commun.* **2014**, *50*, 12434-12446; d) T. Hashimoto, K. Maruoka, *Chem. Rev.* **2015**, *115*, 5366-5412.
- [13] a) C. Bhat, S. G. Tilve, *RSC Adv.* **2014**, *4*, 5405-5452; b) M. I. Calaza, C. Cativiela, *Eur. J. Org. Chem.* **2008**, 3427-3448.
- [14] a) A. Pascual-Escudero, A. de Cózar, F. P. Cossío, J. Adrio, J. C. Carretero, *Angew. Chem. Int. Ed.* **2016**, *55*, 15334-15338; b) K. Liu, Y. Xiong, Z.-F. Wang, H.-Y. Taoa, C.-J. Wang, *Chem. Commun.* **2016**, *52*, 9458-9461.
- [15] a) A. Guerrero-Corella, J. Asenjo-Pascual, T. Janardan Pawar, S. Díaz-Tendero, A. Martín-Sómer, C. Villegas Gómez, J. L. Belmonte-Vázquez, D. E. Ramírez-Ornelas, E. Peña-Cabrera, A. Fraile, D. Cruz Cruz, J. Alemán, *Chem. Sci.* **2019**, *10*, 4346-4351; b) Y. Liu, X. Lv, M. Hou, Y. Shi, W. Guo, *Anal. Chem.* **2015**, *87*, 11475-11483.
- [16] We carried out the reaction at -30 °C but the conversion was very low and the ee value was similar to the obtaining at 4 °C.
- [17] CCDC 1899217 (**3k**) contains the crystallographic data. These data can be obtained free of charge at www.ccdc.cam.ac.uk.
- [18] a) All the optimized structures computed can be visualized and download from <http://dx.doi.org/10.19061/iochem-bd-8-6>; b) M. Álvarez-Moreno, C. de Graaf, N. Lopez, F. Maseras, J. M. Poblet, C. Bo, *J. Chem. Inf. Model.* **2015**, *55*, 95-103.
- [19] Gaussian 09, Revision E.01, M. J. Frisch et al., Gaussian, Inc., Wallingford CT, **2013**.
- [20] I. Fleming, *Frontier Orbitals and Organic Chemical Reactions*, Wiley, London, **1978**.
- [21] For cycloaddition with maleimide, β -nitrostyrene and dimethyl fumarate, see: S. Cabrera, R. Gómez Arrayás, J. C. Carretero, *J. Am. Chem. Soc.* **2005**, *127*, 16394-16395. For cycloaddition with (*E*)-4-phenylbut-3-en-2-one, see: b) J. Hernández-Toribio, R. Gómez Arrayás, B. Martín-Matute, J. C. Carretero, *Org. Lett.* **2009**, *11*, 393-396.
- [22] The importance of pre-association complexes (PAC) was studied in an aminocatalytic case, see: a) E. Arpa M. Frías, C. Alvarado, J. Alemán, S. Díaz-Tendero, *J. Mol. Cat. A.* **2016**, *423*, 308-318; b) F. Aguilar-Galindo, A. M. Tuñón, A. Fraile, J. Alemán, S. Díaz-Tendero, *Theor. Chem. Acc.* **2019**, *138*, 59; c) A. Martín-Sómer, E. M. Arpa, S. Díaz-Tendero, J. Alemán, *Eur. J. Org. Chem.* **2019**, 574-581.
- [23] V. Leen, P. Yuan, L. Wang, N. Boens, W. Dehaen, *Org. Lett.* **2012**, *14*, 6150-6153.

FULL PAPER

Boron Dipyrromethene (BODIPY) as Electron-Withdrawing Group in Asymmetric Copper-Catalyzed [3+2] Cycloadditions for the Synthesis of Pyrrolidine-Based Biological Sensors

Adv. Synth. Catal. **Year**, *Volume*, Page – Page

Thomas Rigotti, Juan Asenjo-Pascual, Ana Martín-Somer, Paula Milán Rois, Marco Cordani, Sergio Díaz-Tendero, Álvaro Somoza, Alberto Fraile,* José Alemán*

